Synthesis, Structure and Magnetic Properties of a Novel Linear Cu^{II}-Trimer Complex

Vladimir Pashchenko,*[a] Bernhard Brendel,[a] Bernd Wolf,[a] Michael Lang,[a] Konstantin Lyssenko,[b] Olga Shchegolikhina,[b] Yulia Molodtsova,[b] Larisa Zherlitsyna,[c] Norbert Auner,*[c] Florian Schütz,[d] Marcus Kollar,[d][‡] Peter Kopietz,[d] and Neil Harrison[e]

Keywords: Copper / Cluster compounds / Sandwich complexes / Magnetic properties

A new hexanuclear copper(II) sandwich complex based on two 10-membered macrocyclic phenylsiloxanolate ligands, $\{Cu_6[(C_6H_5SiO_2)_5]_2(OH)_2(C_{10}H_8N_2)_2\}\cdot 4(DMF)\cdot 3(H_2O)$ (**1**), was synthesized and characterized by single-crystal X-ray diffraction and measurements of the magnetic susceptibility and isothermal magnetization. The cluster compound crystallizes in the triclinic system, space group $P\bar{1}$ (No. 2), with a = 14.925(3) Å, b = 16.745(2) Å, c = 23.053(3) Å, α = 83.079(9)°, β = 84.836(13)°, γ = 65.019(17)°, and Z = 2. The unit cell contains two identical molecules, each consisting of six interacting Cu^{2+} (S = 1/2) ions. Within the molecule, the six Cu^{2+} ions are arranged in two almost linear, parallel trimers. While pairs of oxygen atoms link the Cu^{2+} ions within the trimers, single oxygen atoms residing at the ends of the trimers provide the strongest intertrimer bonds. Magnetic measurements reveal an antiferromagnetic *intra*trimer exchange interaction, J/k_B = 85 K, as the dominant magnetic coupling of the complex. By introducing a weak antiferromagnetic *inter*trimer coupling, J'/k_B = 3.5 K, a satisfactory description of the magnetic behavior over a wide range of temperature and magnetic field is obtained. The departure of the model curves from the data at the lowest available temperature indicates the presence of additional, weak *intra*- and/or *inter*molecular interactions.

Introduction

The synthesis of new magnetic clusters with unprecedented spin topologies is a central topic in the field of molecular magnetism. Among different strategies that have been developed, serendipitous assembly[1] and rational design[2] represent opposite limiting approaches. Following on from the latter route, the rational construction of heptanuclear clusters with high-spin ground states has been reported very recently, starting from hexacyanometalates $[M(CN)_6]^{3-}$ (M = Cr, Fe) and mononuclear complexes bearing a capping ligand.[2]

Moreover, a decanuclear copper(II) cluster, $\{[Cu_6\{(PhSiO_2)_6\}_2]\cdot[Cu(tmpa)CN]_4\}\cdot(PF_6)_4$ (**2**) [tmpa = tris(2-pyridilmethyl)amine], was designed and synthesized by a self-assembly between a hexacopper(II) siloxanolate cage and the monomeric complex $[Cu(tmpa)CN]\cdot(PF_6)$.[3] This cluster compound exhibits interesting magnetic properties with a low-lying S = 5 state arising from a unique spin arrangement.

In the past decade, a widespread series of copper-containing siloxanolate complexes was synthesized and structurally characterized,[4] basically showing two different types of structural features: a sandwich-like molecular structure was found for $\{K_4[\{(RSiO_2)_6\}_2Cu_4]\}\cdot 4(n\text{BuOH})$ [R = Et (**3**),[4a] Ph[4b]] and $\{Cu_6[(PhSiO_2)_6]_2\}\cdot 6(L)$ [L = EtOH (**4**),[4c] L = DMF (**5**)[4d]]. These clusters are composed of two 12-membered (6 Si + 6 O) stereoregular organosiloxanolate fragments, *cis*-$[RSi(O)O^-]_6$, linked together through four or six copper atoms. In contrast, compounds such as $\{Na_4[(PhSiO_2)_{12}Cu_4]\}\cdot 8(n\text{BuOH})$ (**6**),[4e,4f] $\{M_4[(ViSiO_2)_{12}Cu_4]\}\cdot m(n\text{BuOH})$ [M = K, Vi = vinyl, m = 6 (**7**);[4e] M = Na, m = 4 (**8**)[4f]] and $\{Na_4[(EtSiO_2)_{12}Cu_4]\}\cdot 4(n\text{BuOH})$[4g] are based on a 24-membered stereoregular organosiloxanolate fragment $[RSi(O)O^-]_{12}$ (R = Et, Vi, Ph) of tris-*cis*-tris-*trans* configuration and fixed in the "horse saddle" conformation

[a] Physikalisches Institut, J. W. Goethe-Universität Frankfurt, FOR 412,
60438 Frankfurt (M), Germany
Fax: +49-069-798-47250
E-mail: pashchenko@physik.uni-frankfurt.de
[b] A. N. Nesmeyanov Institute of Organoelement Compounds, Russian Academy of Sciences,
117813 Moscow, Russian Federation
[c] Institut für Anorganische Chemie, J. W. Goethe-Universität Frankfurt, FOR 412,
60439 Frankfurt (M), Germany
Fax: +49-069-798-29188
E-mail: auner@chemie.uni-frankfurt.de
[d] Institut für Theoretische Physik, J. W. Goethe-Universität Frankfurt, FOR 412,
60438 Frankfurt (M), Germany
[e] Los Alamos National Laboratory, MS E536,
Los Alamos, NM 87545, USA
[‡] New permanent address: Theoretische Physik III, Universität Augsburg,
86135 Augsburg, Germany
Supporting information for this article is available on the WWW under http://www.eurjic.org or from the author.

by four Cu and four alkaline metal atoms. Investigations of the magnetic properties of the globular tetranuclear complex $\{Na_4[(PhSiO_2)_{12}Cu_4]\}\cdot 8(n\text{BuOH})$ (**6**) and the sandwich-like tetranuclear complex $\{K_4[\{(EtSiO_2)_6\}_2Cu_4]\}\cdot 4(n\text{BuOH})$ (**3**), as well as the hexanuclear sandwich complex $\{Cu_6[(PhSiO_2)_6]_2\}\cdot 6(\text{EtOH})$ (**4**), revealed that the six copper ions in **4** are ferromagnetically coupled with a total spin $S = 3$, whereas strong antiferromagnetic Cu–Cu interactions with an $S = 0$ ground state were detected in the tetranuclear complexes **3** and **6**. These experimental findings prompted us to recrystallize complex **6** with additional ligands that would assemble the molecular unit into a supramolecular structure with new physical properties. Thus, recrystallization of **6**, which contains four sodium ions along with four copper ions, in DMF as solvent and in the presence of 2,2′-bipyridine (bipy), was performed. Unexpectedly, a completely new hexanuclear Cu complex with a sandwich-like structure not containing any alkaline metal ions was obtained.

Here we report the synthesis, structural and magnetic properties of a novel hexacopper(II) siloxanolate cluster compound $\{Cu_6[(PhSiO_2)_5]_2(OH)_2(C_{10}H_8N_2)_2\}\cdot 4(\text{DMF})\cdot 3(H_2O)$, which is unique in that the six Cu^{2+} ions are arranged in two parallel 3-site strings, that is, coupled $S = 1/2$ trimers. A preliminary account of the work has been published in ref.[5]

Results and Discussion

According to Scheme 1, the hexanuclear Cu sandwich complex **1**, which is based on 10-membered *cis*-pentaphenylcyclopentasiloxanolate ligands, was obtained by recrystallization of a tetranuclear Cu complex **6**, which is based on a 24-membered dodecaphenylcyclododecasiloxanolate ligand of tris-*cis*-tris-*trans* configuration possessing the globule-like structure $\{Na_4[(PhSiO_2)_{12}Cu_4]\}\cdot 8(n\text{BuOH})$,[4e,4f] in DMF and in the presence of 2,2′-bipyridine (bipy) at about 30 °C.

Under these experimental conditions, the initial complex **6** underwent a dramatic rebuilding with a formation of complex **1**, no longer containing alkaline ions in yields up to 92%. Crystals of sodium phenylsiloxanolate and of polyhedral phenylsilsesquioxane can easily be separated from the blue crystals of **1** (crystal size ca. 1 mm) and were detected as by-products of the complex formation.

The surprising transformation of complex **6** into **1** is reproducible, but strongly depends on the reaction conditions. The amount of 2,2′-bipyridine is of great importance on product formation. While from the stoichiometric ratio of 1 × complex **6**/4 × bipy in DMF, $\{Cu_6[(PhSiO_2)_5]_2(OH)_2(C_{10}H_8N_2)_2\}\cdot 4(\text{DMF})\cdot 3(H_2O)$ (**1**) is obtained, mixtures of 1 × **6**/2 × bipy in DMF and toluene gave $\{Cu_6[(PhSiO_2)_6]_2\}\cdot 6(\text{DMF})$, and without toluene the complex $\{Cu_6[(PhSiO_2)_5]_2(OH)_2(C_{10}H_8N_2)_2\}\cdot 3(\text{DMF})$ was isolated. Reaction of **6** with bipy in DMF in a molar ration of 1:1 gave $\{Cu_6[(PhSiO_2)_6]_2\}\cdot 6(\text{DMF})$. DMF was not especially dried prior to use. Performing the two months' recrystallization in an open system, even the moisture from air might influence the product formation, resulting in the introduction of different amounts of hydroxy ligands and water into the crystals. All the compounds formed have been fully characterized by single-crystal X-ray analysis and will be published elsewhere.[6] These very complex reaction pathways are currently being investigated in detail in our laboratories.

Crystal Structure of $\{Cu_6[(PhSiO_2)_5]_2(OH)_2(C_{10}H_8N_2)_2\}\cdot 4(\text{DMF})\cdot 3(H_2O)$ (1)

Complex **1** exhibits a sandwich-like structure (Figure 1) and consists of two pentaphenylcyclopentasiloxanolate ligands connected by six Cu^{II} atoms arranged in a $Cu_6O_{10}(OH)_2$ moiety (Figure 2). Notably, this is the first example of a metallasiloxane with an odd number of Si–O units in the siloxanolate rings, which seem to predominantly determine the structural and physical features of the complex.

The two 10-membered siloxanolate $(Si–O)_5$ rings are coaxial and shifted in respect to each other and to the central $Cu_6O_{10}(OH)_2$ segment (Figure 1). The siloxanolate cycles are characterized by an envelope conformation with the deviation of Si(2) or Si(9) atoms from the plane of the remaining silicon atoms by 0.52 and 0.60 Å, respectively. The Ph groups exhibit an all-*cis* arrangement. The Si–O bond lengths vary in the range of 1.591(2)–1.652(2) Å, which is usual for this class of compounds.[7] The $Cu_6O_{10}(OH)_2$ segment is built up of two almost parallel Cu–O_2–Cu–O_2–Cu–

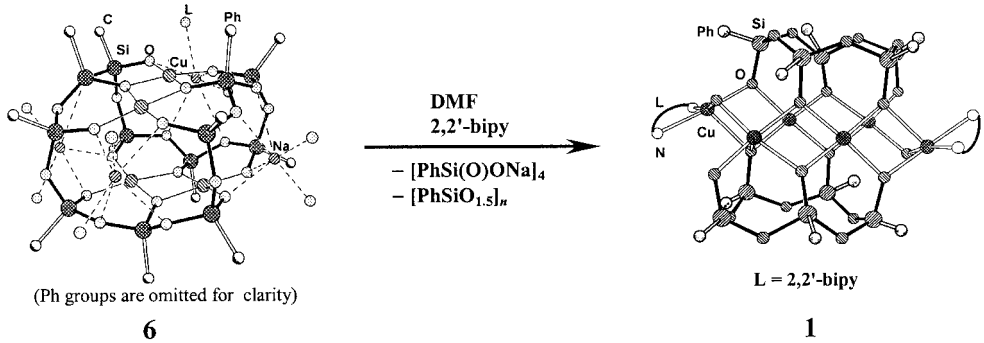

Scheme 1.

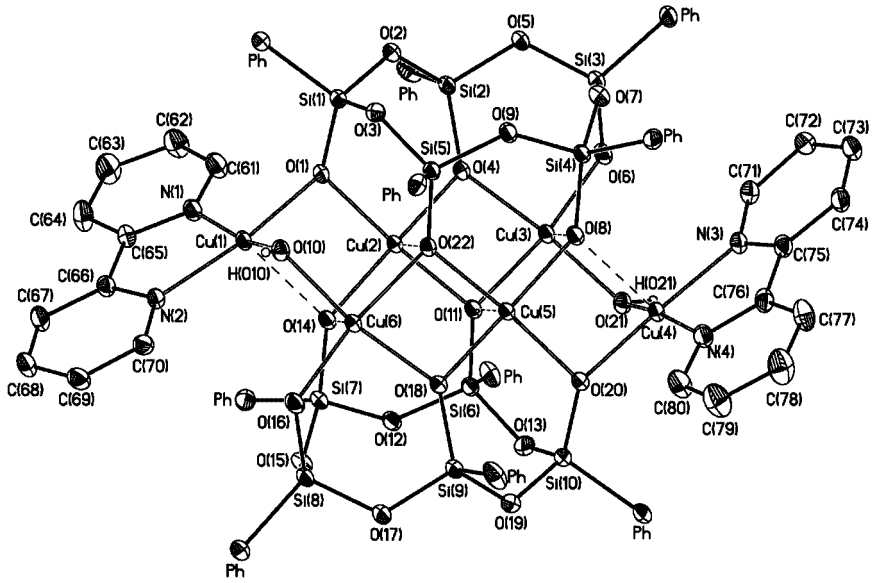

Figure 1. General view of complex **1** (50% probability ellipsoids). Ph groups are omitted for clarity. The dashed lines indicate the apical coordination of copper atoms.

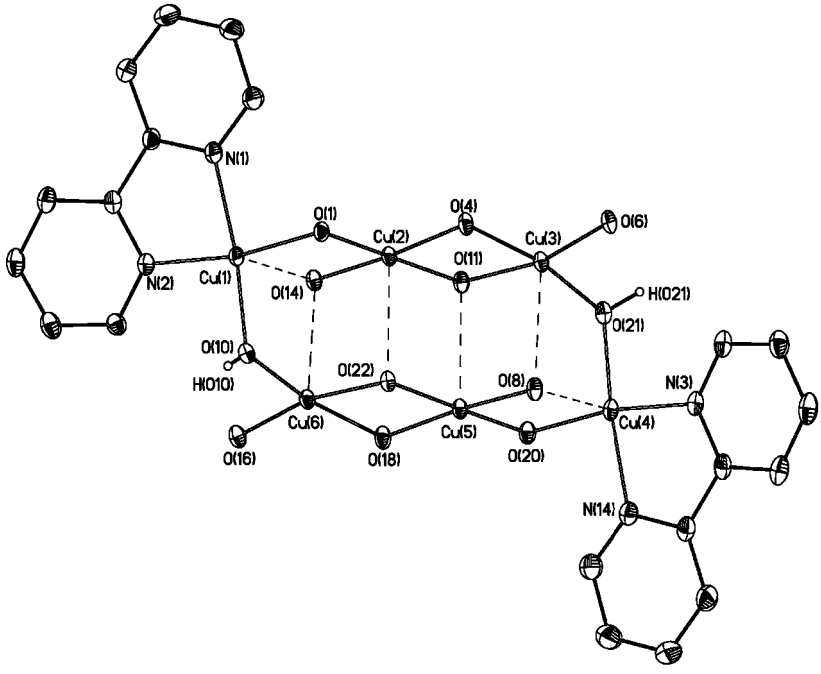

Figure 2. The $Cu_6O_{10}(OH)_2 \cdot bipy_2$ moiety in **1**.

(O,OH) layers. The three copper atoms within the layer form a nearly linear trimer with a Cu–Cu–Cu angle of 173.5(1)° (Figure 2). The nonbonded Cu···Cu distances in the trimer are within the range of 2.9931(6)–3.0310(6) Å, which is significantly longer than corresponding distances described earlier in the sandwich-like copperphenylsiloxanes $\{Cu_6[(PhSiO_2)_6]_2\} \cdot 6(EtOH)$ (**4**),[4c] $\{Cu_6[(PhSiO_2)_6]_2\} \cdot 6(DMF)$ (**5**),[4d] and $\{[Cu_6\{(PhSiO_2)_6\}_2] \cdot [Cu(tmpa)CN]_4\} \cdot (PF_6)_4$ (**2**),[3a] yielding an average value of about 2.82 ± 0.03 Å.

The coordination surrounding of the copper atoms in the layers is different and consists of solely siloxanolate oxygen atoms [for Cu(2), Cu(5)], siloxanolate and hydroxyl oxygen atoms [Cu(3), Cu(6)], or, finally, siloxanolate as well as hydroxyl oxygen atoms and bipyridyl nitrogen atoms [Cu(1), Cu(4)].

Despite the differences in the coordination environment of the copper atoms, all of them exhibit a slightly distorted square-pyramidal (SP) configuration. An analogous configuration of Cu^{II} atoms was found earlier for sandwich-

like (phenylsiloxane)copper compounds **2**, **4**, and **5**. For globular-type copper-containing organosiloxanolates $\{Na_4[(PhSiO_2)_{12}Cu_4]\}\cdot 8(n\text{BuOH})$ (**6**), $\{K_4[(ViSiO_2)_{12}Cu_4]\}\cdot 6(n\text{BuOH})$ (**7**), and $\{Na_4[(ViSiO_2)_{12}Cu_4]\}\cdot 4(n\text{BuOH})$ (**8**), a square-planar configuration was determined.[4e,4f] It should be noted that in compounds **2**, **4**, or **5** the copper–oxygen moieties are organized in cyclic forms and the SP configuration arises from the apical bonding with solvent (**4**, **5**) or organometallic cluster (**2**) molecules. In contrast, for complex **1** the apical positions are occupied by oxygen atoms of the $Cu_6O_{10}(OH)_2$ segment.

The equatorial Cu–O bonds in **1** vary in the range of 1.907(2)–2.013(2) Å (average value 1.95 Å) (Table 1), which is close to the expected values for copper atoms with an SP coordination environment. In the recently reported sandwich-type complex **2**, it was demonstrated that the Cu–O bond lengths in the basal plane for SP [1.909(5)–2.005(4), av. 1.96 Å] and square-planar coordination [1.876(5)–1.922(5), av. 1.90 Å] are different.[3a] The Cu–N bonds in **1** are 1.999(2)–2.015(2) Å long.

Table 1. Selected bond lengths and angles in the $Cu_6O_{10}(OH)_2$ segment of **1**.

Bond lengths [Å]			
Cu(1)–O(1)	1.973(2)	Cu(4)–O(8)	2.182(2)
Cu(1)–O(10)	1.917(2)	Cu(4)–O(20)	1.980(2)
Cu(1)–O(14)	2.242(2)	Cu(4)–O(21)	1.921(2)
Cu(1)–N(1)	2.014(2)	Cu(4)–N(3)	2.016(2)
Cu(1)–N(2)	2.002(2)	Cu(4)–N(4)	2.010(2)
Cu(2)–O(1)	1.961(2)	Cu(5)–O(8)	1.924(2)
Cu(2)–O(4)	1.928(2)	Cu(5)–O(11)	2.572(2)
Cu(2)–O(11)	1.963(2)	Cu(5)–O(18)	1.924(2)
Cu(2)–O(14)	1.923(2)	Cu(5)–O(20)	1.956(2)
Cu(2)–O(22)	2.532(2)	Cu(5)–O(22)	1.952(2)
Cu(3)–O(4)	2.001(2)	Cu(6)–O(10)	1.925(2)
Cu(3)–O(6)	1.907(2)	Cu(6)–O(14)	2.413(2)
Cu(3)–O(8)	2.593(2)	Cu(6)–O(16)	1.916(2)
Cu(3)–O(11)	1.985(2)	Cu(6)–O(18)	1.987(2)
Cu(3)–O(21)	1.925(2)	Cu(6)–O(22)	2.013(2)
Bond angles [°]			
Cu(2)–O(1)–Cu(1)	100.78(7)	Cu(2)–O(14)–Cu(1)	93.09(6)
Cu(2)–O(4)–Cu(3)	99.30(7)	Cu(2)–O(14)–Cu(6)	92.79(6)
Cu(5)–O(8)–Cu(4)	93.37(6)	Cu(1)–O(14)–Cu(6)	84.09(5)
Cu(5)–O(8)–Cu(3)	89.37(6)	Cu(5)–O(18)–Cu(6)	100.61(7)
Cu(4)–O(8)–Cu(3)	82.64(5)	Cu(5)–O(20)–Cu(4)	98.99(7)
Cu(1)–O(10)–Cu(6)	108.60(9)	Cu(4)–O(21)–Cu(3)	110.92(9)
Cu(2)–O(11)–Cu(3)	98.63(7)	Cu(5)–O(22)–Cu(6)	98.72(7)
Cu(2)–O(11)–Cu(5)	89.42(6)	Cu(5)–O(22)–Cu(2)	90.82(6)
Cu(3)–O(11)–Cu(5)	88.66(6)	Cu(6)–O(22)–Cu(2)	87.21(6)

The apical positions of all copper polyhedra in **1** are occupied by siloxanolate oxygen atoms and the bonds are always significantly longer than the equatorial ones. Regarding the Cu(1) and Cu(4) atoms, the apical positions [O(14) and O(8), respectively] are occupied by siloxanolate oxygen atoms of the same layer with the Cu–O bonds being 2.242(2) and 2.182(2) Å long, while for all other copper atoms the apical oxygen atom belongs to the adjacent layer. The apical Cu–O bonds between layers vary in the range of 2.413(2)–2.593(2) Å, the shortest one being the Cu(6)–O(14) bond.

Interestingly, such an architecture of a copper–oxide moiety with Cu–O interlayer interactions is rather rare. Thus, in the series of globular-like copper-containing organosiloxanes **6**, **7**, and **8**, the corresponding interlayer Cu···O distances are in the range of 3.371(5)–3.899(3) Å, which fully excludes any interlayer bonding.

The Cu–O–Cu angles, which mainly determine the magnetochemical behavior of polynuclear clusters, differ within a Cu–O_2–Cu–O_2–Cu–(O,OH) layer and between the layers significantly. For a single layer, these angles are close to 100°, with the exception of one angle, the Cu(1)–O(14)–Cu(2) angle, for example, for the top layer, which is equal to 93.13(6)° (Table 1). In contrast, the Cu–O–Cu angles formed by copper atoms of different layers are closer to 90°, with the exception of two angles at the hydroxy oxygen atoms O(10) and O(21) [108.59(8)° and 110.94(9)°, respectively]. It is interesting that the range of Cu–O–Cu angles of **1** contains all of the corresponding angles typical for other copper-containing organosiloxanes. Thus, Cu–O–Cu angles for sandwich-like (phenylsiloxane)copper compounds **4** and **5** are close to 100°, while in globular-type **6**, **7**, and **8** they are approximately equal to 90°.

The analysis of the crystal packing in **1** revealed that the stacking of the bipyridyl cycles is the only direct intercomplex interaction. Because of the overlap of the π-systems, neighboring complexes are arranged into stacking-bonded chains parallel to the [011] direction (Figure 3). It should be noted that the interplanar distances (3.43 and 3.22 Å) between the bipyridyl ligands are rather short[8] and a significant π-orbital overlap between adjacent complexes can be expected.

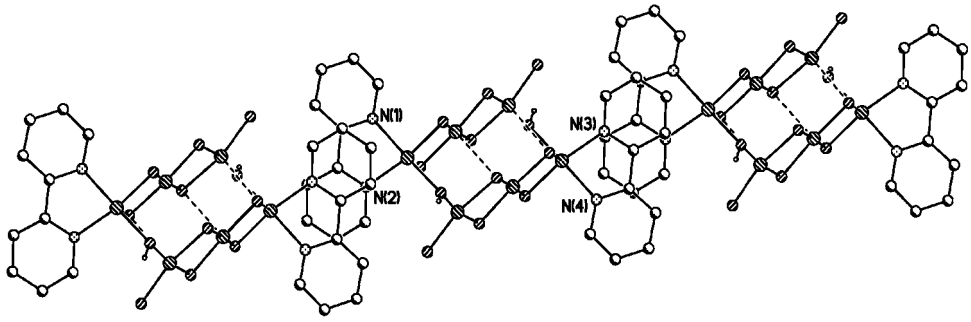

Figure 3. Illustration of the stacking-bonded chains in **1**.

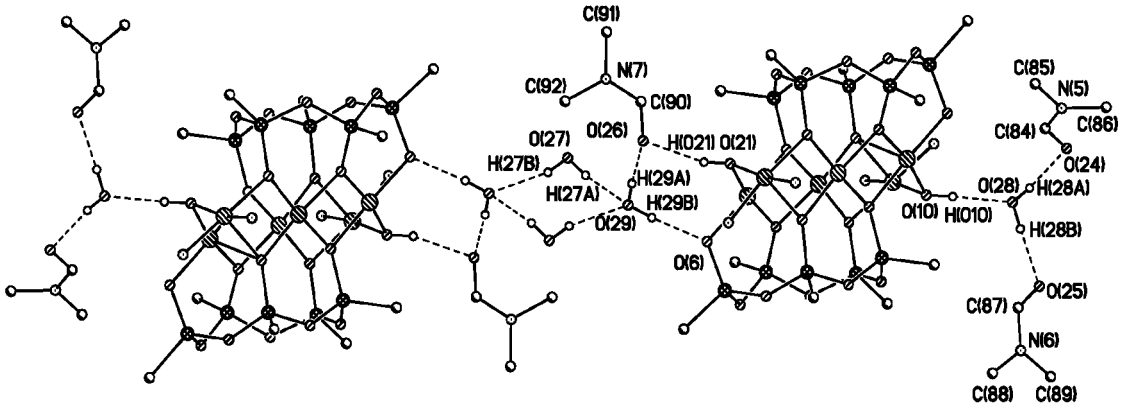

Figure 4. The O–H···O mediated bridging of adjacent complexes in crystals of **1**.

Additionally, the complexes in **1** are connected by intermolecular O–H···O bonds [O···O 2.717(3)–2.894(3) Å] of solvate water molecules (Figure 4). The combination of H-bonding and stacking interactions results in a layered supramolecular arrangement in the crystal.

Magnetic Properties

Magnetic susceptibility and magnetization measurements were performed on polycrystalline samples of $\{Cu_6[(PhSiO_2)_5]_2(OH)_2(C_{10}H_8N_2)_2\}\cdot 4(DMF)\cdot 3(H_2O)$ (**1**). The data were corrected for the contribution of the sample holder and for the diamagnetic core contribution. Notably, the temperature-independent diamagnetic contribution of $\chi_{dia} = -2\times10^{-3}$ cm^3/mol, determined by analyzing the high-temperature magnetic behavior, is in reasonable agreement with the core contribution of $\chi_{core} = -1.7\times10^{-3}$ cm^3/mol calculated by using tabulated values for Pascal's constants.[9]

Figure 5 shows the susceptibility $\chi(T) = M(T)/B$ of complex **1** in a representation $\chi^{-1}(T)$ versus T, where M denotes the magnetic moment of the sample (see also ref.[5]). The data were found to be reversible upon cooling and heating, with no indications of hysteretic behavior. Moreover, no sign of long-range magnetic ordering was observed in the temperature range under investigation.

Figure 5 discloses, to a good approximation, two linear regimes of $\chi^{-1}(T)$ that are separated by a broad crossover range. In an attempt to set up a simple model, capable of describing the main feature of the magnetic susceptibility, these linear sections can be assigned to Curie–Weiss-like temperature dependencies $\chi(T) = C_i\times(T + \theta_i)^{-1}$, with different Curie constants C_i and Weiss temperatures θ_i for the low- (i = LT) and high- (i = HT) -temperature range. At high temperatures of 100–300 K, the best fit reveals C_{HT} = 5.25 cm^3 K/mol and θ_{HT} = 47 K. This Curie constant is consistent with the presence of six Cu^{2+} ions per molecule (two molecules per unit cell) yielding a spin-only value of C_{HT} = 4.96 cm^3 K/mol. The latter number is based on an average spectroscopic g value of 2.09 ± 0.05, as determined by our ESR measurements operated at X- and Q-band frequencies. The positive Weiss constant indicates a dominant antiferromagnetic spin–spin interaction in the high-temperature regime.

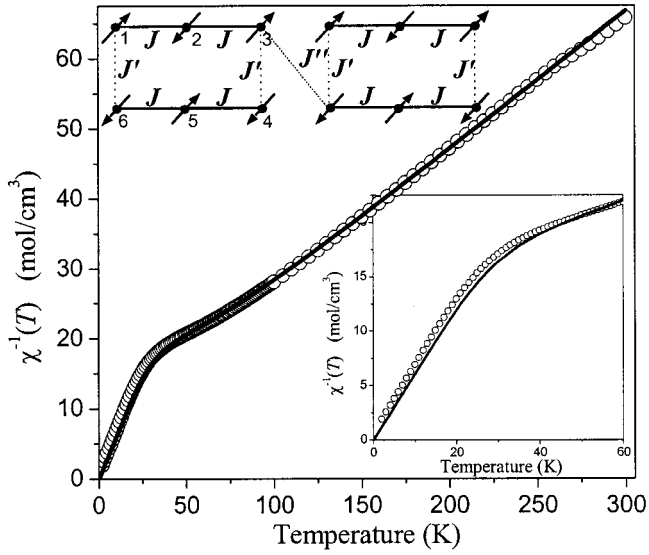

Figure 5. Temperature dependence of the inverse magnetic susceptibility of complex **1** for temperatures 2–300 K. The data have been taken at a magnetic field of 0.05 T. The solid line corresponds to the best fit for the model of isolated, linear S = 1/2 trimers with an antiferromagnetic intratrimer exchange coupling constant J/k_B = 85 K, i.e. $J' = J'' = 0$ in the scheme for the exchange coupling interactions of two adjacent molecules indicated in the upper left of the figure. The inset shows the low-temperature part on expanded scales.

From the linear behavior of $\chi^{-1}(T)$ versus T at low temperatures, that is, in the range 2–15 K, a Curie constant of C_{LT} = 1.61 cm^3 K/mol and an antiferromagnetic Weiss temperature as small as θ_{LT} = 1.05 K were found. A reduction of the Curie constant by a factor close to 3 indicates that the low-temperature magnetic system behaves essentially like an effective "2-spin" S = 1/2 configuration per molecule. In fact, in this case, a Curie constant of 1.65 cm^3 K/mol (for g = 2.09) is expected, which is very close to the C_{LT} value derived from the experiment.

Thus, the magnetic susceptibility of the present hexanuclear complex **1** is reminiscent of that observed in a variety

of systems containing largely isolated trimers.[10,11] This suggests that the dominant magnetic coupling is provided by an *intra*trimer Cu–Cu exchange interaction J within the 3-site Cu strings (cf. the coupling scheme given in the inset of Figure 5).

In a first approach, which has been discussed also in ref.[5], we therefore consider isolated trimers with a uniform isotropic Heisenberg *intra*trimer exchange coupling constant J and an isotropic g factor described by the spin Hamiltonian given in Equation (1).

$$\hat{H}_3 = J(\hat{\boldsymbol{S}}_1\cdot\hat{\boldsymbol{S}}_2 + \hat{\boldsymbol{S}}_2\cdot\hat{\boldsymbol{S}}_3) - g\mu_B\boldsymbol{B}\cdot(\hat{\boldsymbol{S}}_1 + \hat{\boldsymbol{S}}_2 + \hat{\boldsymbol{S}}_3) \quad (1)$$

The energy spectrum of Equation (1) consists of a doublet ground state separated from an excited doublet and quartet by an energy gap $\Delta = J$ and $3J/2$, respectively (see Figure 6). In Figure 6 the spin states of the isolated trimer are labeled according to the eigenvalues of the square of the total spin operator $\hat{\boldsymbol{S}}_{123} = \hat{\boldsymbol{S}}_1 + \hat{\boldsymbol{S}}_2 + \hat{\boldsymbol{S}}_3$, $\hat{\boldsymbol{S}}_{456} = \hat{\boldsymbol{S}}_4 + \hat{\boldsymbol{S}}_5 + \hat{\boldsymbol{S}}_6$ (the coupling scheme of Figure 5) and an intermediate coupling quantum number, S_{13} and S_{46}, defined through the relations $\hat{\boldsymbol{S}}_{13} = \hat{\boldsymbol{S}}_1 + \hat{\boldsymbol{S}}_3$ and $\hat{\boldsymbol{S}}_{46} = \hat{\boldsymbol{S}}_4 + \hat{\boldsymbol{S}}_6$, respectively.

From the partition function the magnetic susceptibility can be derived in a straightforward way yielding Equation (2), where $x = \exp(-J/2k_BT)$.

$$\chi(T) = \frac{N\mu_B^2g^2}{k_B}\cdot\frac{1}{4T}\cdot\frac{1 + x^2 + 10x^3}{1 + x^2 + 2x^3} \quad (2)$$

The result for the magnetization of the isolated linear trimer can be written as Equation (3), where $h = g(\mu_B/k_B)B$.

$$M(T,h) = N\mu_Bg\cdot\frac{1}{2}\cdot\frac{(1 + x^2 + x^3)s_1 + 3x^3s_3}{(1 + x^2 + x^3)c_1 + x^3c_3} \quad (3)$$

We have used the following shorthand notations: $c_1 = \cosh(h/2T)$, $c_3 = \cosh(3h/2T)$, $s_1 = \sinh(h/2T)$, and $s_3 = \sinh(3h/2T)$. In the limit $J\rightarrow\infty$ or $T << J/k_B$, that is, $x\rightarrow 0$, the trimer is locked into a spin-1/2 state and $M(T,h)$ reduces to the spin-1/2 Brillouin function $B_{1/2}(T,h) = (1/2)\tanh(h/2T)$. On the contrary, for vanishing exchange coupling J or $T >> J/k_B$, that is, for $x\rightarrow 1$, the spins of the trimer are independent and $M(T,h)$ can easily be shown to be equivalent to $3B_{1/2}(T,h)$.

Fitting Equation (2) to the susceptibility data in Figure 5 for temperatures between 300 and 25 K, we find a good overall agreement (solid line in Figure 5) for an antiferromagnetic *intra*trimer exchange coupling constant of $J/k_B = 85\pm1$ K (see also ref.[5]). Figure 5 demonstrates that the simple trimer model according to Equation (1) covers the main features of the susceptibility, in particular the increase of the slope of $\chi^{-1}(T)$ by a factor of 3, that is, a reduction of the Curie constant by 2/3, upon cooling. However, a closer look at the low-temperature behavior in Figure 5 (cf. inset) discloses deviations of the model curve from the data, indicating the presence of additional, weaker interactions such as the intertrimer (J') and/or intermolecular couplings (J'') indicated in Figure 5.

A finite trimer–trimer interaction can, indeed, be expected because of the presence of the hydroxy oxygen atoms O(10) and O(21), which may provide an exchange path between the terminal Cu^{II} atoms of adjacent trimers (see Figure 2). Likewise, weak trimer–trimer interactions can arise through the apical oxygen atoms O(14), O(22), O(11), and O(8). Because the latter exchange paths involve rather long Cu–O bonds ranging from 2.413 to 2.593 Å, we expect their coupling strength to be much weaker than those of the above Cu(1)–O(10)–Cu(6) and Cu(3)–O(21)–Cu(4) bonds (cf. Table 1). In a second step we thus model the trimer–trimer interactions by introducing the coupling constant J' that links the ends of the linear trimers within the molecule (cf. the coupling scheme indicated in the upper left of Figure 5).

The resulting Hamiltonian of such an isolated 6-spin $S = 1/2$ assembly, that is, two coupled trimers, then reads as Equation (4).

$$\hat{H}_6 = J(\hat{\boldsymbol{S}}_1\cdot\hat{\boldsymbol{S}}_2 + \hat{\boldsymbol{S}}_2\cdot\hat{\boldsymbol{S}}_3 + \hat{\boldsymbol{S}}_4\cdot\hat{\boldsymbol{S}}_5 + \hat{\boldsymbol{S}}_5\cdot\hat{\boldsymbol{S}}_6) + J'(\hat{\boldsymbol{S}}_1\cdot\hat{\boldsymbol{S}}_6 + \hat{\boldsymbol{S}}_3\cdot\hat{\boldsymbol{S}}_4) - g\mu_B\boldsymbol{B}\cdot(\hat{\boldsymbol{S}}_1 + \hat{\boldsymbol{S}}_2 + \hat{\boldsymbol{S}}_3 + \hat{\boldsymbol{S}}_4 + \hat{\boldsymbol{S}}_5 + \hat{\boldsymbol{S}}_6) \quad (4)$$

As a consequence of the finite trimer–trimer coupling, the degeneracy of the $S = 1/2$ ground state doublets for the isolated trimers within the molecule is lifted and a singlet ($S = 0$) ground state (for an antiferromagnetic coupling $J' > 0$) is formed, which is separated from the first excited triplet ($S = 1$; $M = 1, 0, -1$) state by a zero-field gap of $(8/9)|J'|$, up to higher order corrections in J'/J (see Figure 6). In case of a ferromagnetic coupling $J' < 0$, the order of the low-lying singlet and triplet states is reversed.

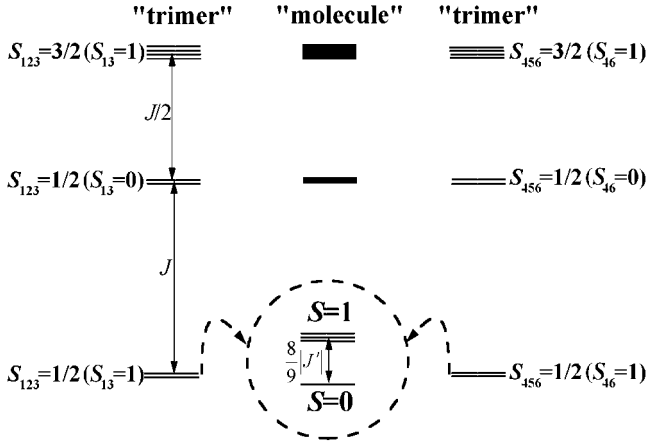

Figure 6. Ground-state splitting of two trimers within the molecule because of antiferromagnetic intertrimer coupling. The spin states of the isolated trimers are labeled as $S(S^*)$. S is the total spin and $S^* = S_1 + S_3$ or $S_4 + S_6$, respectively.

For the magnetic susceptibility, a perturbative approach for $|J'| << |J|$ yields Equation (5), where $x = \exp(-J/2k_BT)$ and $y = \exp(-2J'/9k_BT)$.

$$\chi(T) = \frac{N\mu_B^2g^2}{k_B}\cdot\frac{1}{2T}\cdot\frac{(1 + x^2 + 2x^3)(1 + x^2 + 10x^3) + y - 1}{(1 + x^2 + 2x^3)^2 + (y^{-3} + 3y)/4 - 1} \quad (5)$$

The magnetization is given by Equation (6), where the same shorthands as in Equation (3) are used.

$$M(T,h) = N\mu_B g \cdot \frac{[(1 + x^2 + x^3)c_1 + x^3c_3][(1 + x^2 + x^3)s_1 + 3x^3s_3] + (y - 1)c_1s_1}{[(1 + x^2 + x^3)c_1 + x^3c_3]^2 + c_1^2(y - 1) + (y^{-3} - y)/4} \quad (6)$$

Equations (5) and (6) can be checked by comparison with numerical diagonalization for the full model. At least up to $|J'/J| \leq 0.1$, we obtain excellent agreement with the exact result. For $J' = 0$, Equations (5) and (6) result in twice the susceptibility and the magnetization of an isolated trimer given in Equations (2) and (3), respectively, as expected. Note that the influence of J' on susceptibility is rather small and deviations from the pure trimer model become visible only at low temperatures. To visualize the effect of a weak intertrimer coupling on the susceptibility more clearly, the data together with the model curves for the isolated and coupled trimers are plotted in Figure 7 in a representation χT versus T.

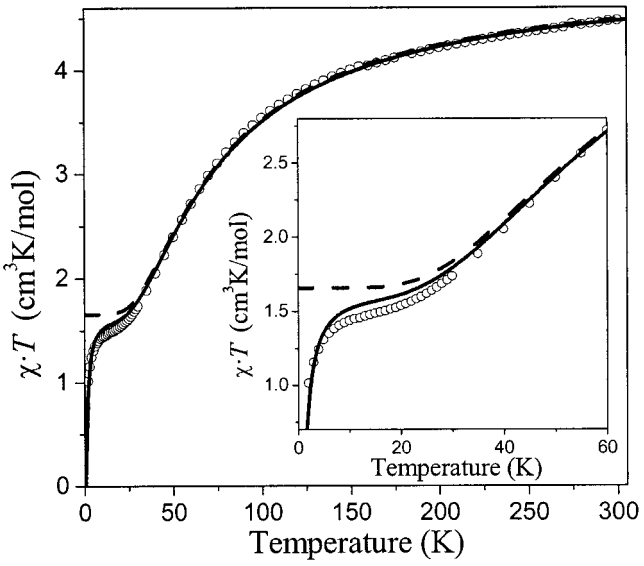

Figure 7. Magnetic susceptibility data of complex **1** taken at a field of 0.05 T plotted as χT versus T. The inset shows the low-temperature behavior on expanded scales. The dashed lines correspond to the best fit for the isolated linear trimer model with $J/k_B = 85$ K; the solid lines are the result of the model for antiferromagnetically coupled trimers with $J/k_B = 85$ K and $J'/k_B = 3.5$ K.

Figure 7 shows the best fit for weakly coupled trimers with an *intra*trimer coupling $J/k_B = 85$ K and a weak antiferromagnetic *inter*trimer coupling $J'/k_B = 3.5$ K, while the dashed line indicates the results for the isolated trimer model with $J/k_B = 85$ K. Figure 7 clearly demonstrates that the incorporation of a finite intertrimer coupling J' improves the fit considerably at low temperatures, although small deviations of the model curve from the data are still visible below 30 K. This is most likely due to the presence of additional, weaker interaction pathways between the copper atoms of adjacent trimers such as the coupling through the apical oxygen atoms mentioned above. As has been discussed by Zaspel et al.,[12] who carried out a high-temperature series expansion for the Heisenberg model with the intertrimer coupling constants as expansion parameters, the low-temperature behavior of such a generalized coupled-trimer model depends on the sign combinations and magnitudes of the intertrimer coupling constants. As the above coupled-trimer model covers the main properties of the susceptibility of complex **1** in the temperature range under investigation, we refrain from introducing additional coupling constants at the present stage. This also includes the introduction of a finite intermolecular coupling J'', which does not significantly improve the quality of the fit. Thus, we conclude that the temperature dependence of the magnetic susceptibility of complex **1** can be satisfactorily described by coupled trimers with an average antiferromagnetic trimer–trimer interaction $J'/k_B = 3.5$ K.[13]

Further support for this assignment can be gained from the results of isothermal magnetization measurements (see Figure 8). The figure also shows the calculated magnetization curves for the above-discussed models of isolated [dashed lines, Equation (3)] and antiferromagnetically coupled [solid lines, Equation (6)] trimers. Figure 8 clearly demonstrates that, for temperatures below 20 K, the isolated-trimer model progressively departs from the experimental data. On the other hand, a very good description of the magnetization curves, except the data taken at the lowest temperature of 2 K, is achieved by the model of antiferromagnetically coupled trimers, with the best fit obtained for the parameters $J/k_B = 85$ K and $J'/k_B = 3.4 \pm 0.5$ K. This model also explains the high-field data taken at $T = 4.2$ K, showing a saturation of the magnetization at a value close to $2\mu_B$ per molecule, as expected for two weakly coupled $S = 1/2$ (trimer) states. However, deviations of the above model from the experimental data become visible at the lowest temperature of 2 K for fields $B \geq 2$ T. This indicates the presence of additional weak *intra*- and/or *inter*molecular interactions giving rise to a more complicated low-energy spectrum of this cluster compound. We note that for

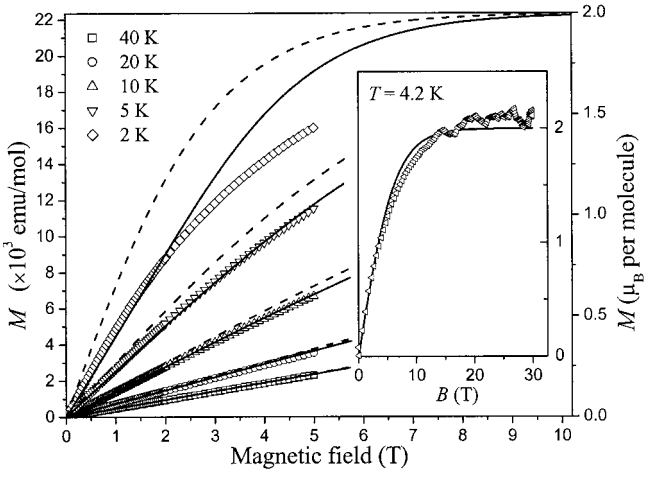

Figure 8. Isothermal magnetization measurements in dc fields from 0 to 5 T (main panel) and pulsed fields from 0 to 30 T (inset) at varying temperatures as indicated in the figure. The right scales of the main panel and inset are given in units of μ_B per molecule. The dashed and solid lines correspond to the model curves for isolated and antiferromagnetically coupled trimers, respectively, with the coupling parameters given in the text.

a ferromagnetic coupling $J' < 0$, as suggested in ref.[5], the initial slope of the corresponding magnetization curves even exceeds that for the isolated trimers (broken lines), which would make the fit worse.

Conclusions

This paper reports on the synthesis, X-ray crystal structure, and magnetic properties of a new hexanuclear copper(II) siloxanolate cluster compound **1**, $\{Cu_6[(C_6H_5SiO_2)_5]_2(OH)_2(C_{10}H_8N_2)_2\}\cdot 4(DMF)\cdot 3(H_2O)$. This molecular complex differs from the known hexacopper(II) cluster compounds in its unique $S = 1/2$ trimer arrangement: each molecule contains two linear oxygen-bridged three-site Cu^{II} strings that are parallel to each other.

According to magnetic measurements, an antiferromagnetic *intra*trimer coupling constant marks the dominant magnetic coupling in this complex. Indeed, an $S = 1/2$ Heisenberg trimer model with an isotropic antiferromagnetic exchange coupling $J/k_B = 85$ K covers the main features of the magnetic susceptibility, namely the formation of an effective $S = 1/2$ low-temperature trimer state. This model, however, fails to describe adequately the magnetic behavior at low temperatures. The model can be improved significantly by introducing a weak antiferromagnetic *inter*trimer interaction $J'/k_B = 3.5$ K, giving rise to a singlet ($S = 0$) ground state and a nearby [with energy gap $\Delta = (8/9)|J'|$] excited triplet ($S = 1$) state for the molecules. The small deviations of the model curves from the experimental data at low temperatures indicate the action of additional, weaker magnetic interaction pathways such as additional couplings between the copper atoms of adjacent trimers within a single molecule or a finite *inter*molecular coupling. The latter might originate in the overlap of π-orbitals from the bipyridine groups of adjacent molecules.

Experimental Section

Synthesis of the Hexanuclear Copper Complex $\{Cu_6[(PhSiO_2)_5]_2(OH)_2(C_{10}H_8N_2)_2\}\cdot 4(DMF)\cdot 3(H_2O)$ (1): A solution of complex **6** (0.5 g, 0.25 mmol), which was prepared as described in ref.[4f], was made up of DMF (25 mL) and 2,2′-bipyridine (0.156 g, 1 mmol) in DMF (25 mL). Within two months, blue crystals precipitated. They were isolated and dried under vacuum (1 Torr, 50 °C). Yield: 0.33 g (91.7%). Anal.: Calcd. for $\{Cu_6[(PhSiO_2)_5]_2(OH)_2(C_{10}H_8N_2)_2\}\cdot(DMF)$, $[C_{83}H_{75}Si_{10}Cu_6N_5O_{23}]$, %: C 45.88, H 3.49, Si 12.93, Cu 17.55, N 3.22; found, %: C 46.14, H 4.28, Si 12.38, Cu 17.34, N 2.39. Notably, metallasiloxane compounds always contained some amount of solvate molecules. During the separation of the crystals from the mother liquor and during the drying process in vacuo, some of the solvate molecules evaporated. Consequently, the molecular formula determined by X-ray analysis of a single crystal differed from the molecular formula obtained by an elemental analysis including solvate ligands. The composition of the hexanuclear complex **1** was determined by single-crystal X-ray analysis as $\{Cu_6[(PhSiO_2)_5]_2(OH)_2(C_{10}H_8N_2)_2\}\cdot 4(DMF)\cdot 3(H_2O)$ and by elemental analysis as $\{Cu_6[(PhSiO_2)_5]_2(OH)_2(C_{10}H_8N_2)_2\}\cdot(DMF)$. Magnetic measurements were performed with crystals directly isolated from the mother liquor and thus corresponding to the formula determined by X-ray analysis.

X-ray Crystallography: The crystallographic data for complex **1**, $\{Cu_6[(PhSiO_2)_5]_2(OH)_2(C_{10}H_8N_2)_2\}\cdot 4(DMF)\cdot 3(H_2O)$, are listed in Table 2. The X-ray diffraction measurements were performed employing a Smart CCD diffractometer (Mo-K_α radiation, graphite-monochromator, ω-scan technique). A numerical absorption correction was carried out based on six indexed crystal faces. The transmission factor ranges from 0.609 to 0.784. The structure was solved by direct methods and refined by full-matrix least squares against F^2 in the anisotropic (H-atoms isotropic) approximation, using the SHELXTL-97 package.[14] The H positions of the Ph groups were calculated from a geometrical point of view, while the methyl and hydroxyl groups and the hydrogen atoms of water molecules were located in the Fourier electron-density synthesis. CCDC-269903 contains the supplementary crystallographic data for this paper. These data can be obtained free of charge from The Cambridge Crystallographic Data Centre via www.ccdc.cam.ac.uk/data_request/cif.

Table 2. Crystallographic data for **1**.

	1
Empirical formula	$C_{92}H_{102}Cu_6N_8O_{29}Si_{10}$
Crystal dimensions [mm]	$0.23 \times 0.26 \times 0.32$
M	2445.96
T [K]	146(2)
Crystal system, space group	triclinic, $P\bar{1}$
a [Å]	14.925(3)
b [Å]	16.745(2)
c [Å]	23.053(3)
α [°]	83.079(9)
β [°]	84.836(13)
γ [°]	65.019(17)
V [Å^3], Z	5179.6(14), 2
μ [cm^{-1}]	14.06
$F(000)$	2512
$\rho_{calcd.}$ [g/cm^{-3}]	1.568
$2\theta_{max}$ [°]	60
No. of reflections measured (R_{int})	101967 (0.0466)
No. of independent reflections	29492
No. of reflections with $I > 2\sigma(I)$	20220
No. of parameters	1330
R_1	0.0390
wR_2	0.0901
GOF	1.061
Max./min. peak [e/Å^{-3}]	0.545/–0.563

Magnetic Susceptibility and Magnetization Measurements: Variable-temperature magnetic susceptibility measurements in the temperature range 2–300 K and magnetic fields up to 5 T were carried out using a Quantum Design SQUID magnetometer MPMS-XL. These measurements were complemented by isothermal magnetization runs at temperatures between 2 and 40 K for fields up to 5 T. In addition, pulsed-field magnetization measurements up to 35 T were performed at the NHMFL, Los Alamos, using a wire-wound extraction magnetometer.

Supporting Information (see also footnote on the first page of this article): Figures of the crystal packing (Figures S1–S4) and ESR spectrum of polycrystalline sample (Figure S5) for complex **1**.

Acknowledgments

The work was supported by the DFG (Forschergruppenprogramm "Spin- und Ladungskorrelationen in niedrigdimensionalen metall-

organischen Festkörpern", FOR412). We thank J. Bats (Institut für Anorganische Chemie, J. W. Goethe-Universität Frankfurt) for collection of the X-ray data.

[1] R. E. P. Winpenny, *J. Chem. Soc., Dalton Trans.* **2002**, 1.
[2] a) T. Mallah, C. Auberger, M. Verdaguer, P. Veillet, *J. Chem. Soc., Chem. Commun.* **1995**, 61; b) A. Scuiller, T. Mallah, M. Verdaguer, A. Nivorozkhin, J.-L. Tholence, P. Veillet, *New J. Chem.* **1996**, *20*, 1; c) G. Rogez, A. Marvilliers, E. Rivière, J.-P. Audière, F. Lloret, F. Varret, A. Goujon, N. Mendenez, J.-J. Girerd, T. Mallah, *Angew. Chem.* **2000**, *112*, 3007–3009; *Angew. Chem. Int. Ed.* **2000**, *39*, 2885.
[3] a) G. L. Abbati, A. Caneschi, A. Cornia, A. C. Fabretti, Yu. A. Pozdniakova, O. I. Shchegolikhina, *Angew. Chem. Int. Ed.* **2002**, *41*, 4517–4520; b) G. L. Abbati, A.-L. Barra, A. Caneschi, A. Cornia, A. Fabretti, D. Gatteschi, Yu. A. Pozdniakova, O. I. Shchegolikhina, *C. R. Chim.* **2003**, *6*, 645–656.
[4] a) V. A. Igonin, S. V. Lindeman, Yu. T. Struchkov, Yu. A. Molodtsova, O. I. Shchegolikhina, A. A. Zhdanov, *Izv. Akad. Nauk, Ser. Khim.* **1993**, *4*, 752; [English translation: *Russ. Chem. Bull.* **1993**, *42*, 718]; b) O. Shchegolikhina, Yu. Pozdniakova, Yu. Molodtsova, I. Blagodatskhih, D. Katsoulis, *Abstracts of XII International Symposium on Organosilicon Chemistry*, **1999**, May 23–27, Sendai, Japan, P180, p. 234; c) E. Rentschler, D. Gatteschi, A. Cornia, A. C. Fabretti, A.-L. Barra, O. I. Shchegolikhina, A. A. Zhdanov, *Inorg. Chem.* **1996**, *35*, 4427–4431; d) S. V. Lindeman, O. I. Shchegolikhina, Yu. A. Molodtsova, A. A. Zhdanov, *Acta Crystallogr., Sect. C* **1997**, *53*, 305–309; e) V. A. Igonin, S. V. Lindeman, Yu. T. Struchkov, O. I. Shchegolikhina, A. A. Zhdanov, Yu. A. Molodtsova, I. V. Razumovskaya, *Organomet. Chem. USSR* **1991**, *4*, 672; f) Yu. A. Molodtsova, Yu. A. Pozdniakova, K. A. Lyssenko, I. V. Blagodatskikh, D. E. Katsoulis, O. I. Shchegolikhina, *J. Organomet. Chem.* **1998**, *571*, 31; g) C. Zucchi, M. Mattioli, G. Gavioli, M. Moret, A. Sironi, R. Ugo, M. Pizzotti, O. I. Shchegolikhina, G. Pályi, *Eur. J. Inorg. Chem.* **2000**, 1327–1331.
[5] V. A. Pashchenko, B. Brendel, B. Wolf, M. Lang, M. Kollar, F. Schütz, P. Kopietz, Y. Molodtsova, O. Shchegolikhina, N. Auner, *J. Magn. Magn. Mater.* **2004**, *272–276*, e755.
[6] Yu. Molodtsova, L. Zherlitsyna, J. Bats, M. Bolte, V. Pashchenko, N. Auner, O. Shchegolikhina, manuscript in preparation.
[7] Yu. T. Struchkov, S. V. Lindeman, *J. Organomet. Chem.* **1995**, *488*, 9.
[8] E. A. Meyer, R. K. Castellano, F. Diederich, *Angew. Chem. Int. Ed.* **2003**, *42*, 1210.
[9] a) E. König, "Magnetic Properties of Coordination and Organo-Metallic Transition Metal Compounds", in *Landolt-Börnstein, Neue Serie*, Springer, Berlin, **1966**, vol. II/2, pp. 1–16; b) R. Boča, *Theoretical Foundations of Molecular Magnetism*, vol. 1 ("Current Methods in Inorganic Chemistry"), Elsevier, Amsterdam, **1999**, appendix 4.
[10] K.-F. Hsu, S.-L. Wang, *Inorg. Chem.* **2000**, *39*, 1773–1778.
[11] a) P. King, R. Clérac, C. E. Anson, C. Coulon, A. K. Powell, *Inorg. Chem.* **2003**, *42*, 3492–3500; b) J. L. Manson, J. Gu, J. A. Schlueter, H. H. Wang, *Inorg. Chem.* **2003**, *42*, 3950–3955.
[12] a) C. E. Zaspel, G. V. Rubenacker, S. L. Hutton, J. E. Drumheller, R. S. Rubins, R. D. Willet, M. R. Bond, *J. Appl. Phys.* **1988**, *63*, 3028; b) M. R. Bond, R. D. Willet, R. S. Rubins, P. Zhou, C. E. Zaspel, S. L. Hutton, J. E. Drumheller, *Phys. Rev. B* **1990**, *42*, 10280.
[13] In ref.[5], a weak ferromagnetic trimer–trimer coupling $J'/k_B = -7$ K has been claimed from the temperature evolution of the absorption signal in a preliminary ESR study. For such a ferromagnetic coupling $J' < 0$, the order of the low-lying singlet–triplet states in the energy spectrum in Figure 6 is just reversed, resulting in an $S = 1$ ground state. In the presence of additional weak anisotropies in the exchange couplings, which can be expected for the present system, the selection rule is no longer valid, enabling transitions between the singlet and triplet states to be observed by ESR measurements. As a result, the ESR studies are not very sensitive to the difference between a ferromagnetic and an antiferromagnetic coupling, unless the data are available for covering the low-temperature range of the order of $(1/2)J'/k_B$.
[14] G. M. Sheldrick, *SHELXS-97 and SHELXL-97, Programs for the determination and refinement of crystal structures*, University of Göttingen, Germany, **1997**.

Received: June 19, 2005
Published Online: September 27, 2005

